UDC 528.852.1:004.932 **doi:** https://doi.org/10.20998/2522-9052.2025.2.09

Sergii Kryvenko[1], Vladimir Lukin[1], Boban Bondzulic[2], Nenad Stojanovic[2]

[1] National Aerospace University, Kharkiv, Ukraine
[2] University of Defence in Belgrade, Belgrade, Serbia

COMPRESSION OF NOISY GRAYSCALE IMAGES WITH COMPRESSION RATIO ANALYSIS

Abstract. The object of the study is the process of compressing noisy images in a lossy manner by better portable graphics (BPG) encoder. **The subject of the study** is the method for adaptive selection of the coder parameter Q depending on noise intensity and image complexity. **The goal of the study** is to consider the basic characteristics of lossy compression of remote sensing images contaminated by additive white Gaussian noise with giving recommendations of preferable Q setting. **Methods used:** numerical simulation, verification for test images. **Results obtained:** 1) the dependencies of compression ratio on Q are monotonically increasing functions; 2) their characteristics are strongly dependent on noise intensity and image complexity; 3) dependencies of logarithm of CR on Q contain information on possible existence and position of optimal operation point for compressed noisy images; 4) compression ratios for large Q contain information on image complexity with low sensitivity to noise presence and intensity; 5) it is possible to get useful information from dependences of compression ratio on Q. **Conclusions:** the results of this research allow: 1) estimating image complexity; 2) adapting Q to noise intensity and image complexity.

Keywords: lossy compression; better portable graphics; noise intensity; image complexity.

Introduction

Modern imaging systems produce a great amount of image data in remote sensing [1], medical diagnostics [2], social networking [3], military [4], ecological monitoring, agriculture [5], etc. One tendency is the increase of image average size due to better resolution of new sensors and the use of more components as this happens in multispectral [4, 5] and hyperspectral [6] imaging. Then, one might run into problems with image storage on-board or on-land as well as with data transferring via communication lines with a limited bandwidth [5-7]. Note that lossless image compression [7, 8] is often unable to satisfy requirements to compression ratio (CR) that occurs to be too small and not variable. These are the reasons why lossy compression has become popular [6, 8, 9]. Lossy compression introduces inevitable distortions and they increase if a desired CR is larger [6, 9]. Then, in practice, one has to provide some compromise between introduced distortions (a compressed images quality) and CR [9, 10].

There are several ways to reaching the compromise. First, it is possible to find a coder providing the best rate/distortion characteristics for a considered type of images. In this paper, we analyze a better portable graphics (BPG) encoder [11-13] that has shown itself to be one of the best possessing several advantages [11]. Second, it is quite easy to provide a desired CR if this is of prime importance [13]. Third, it is also quite easy to provide a desired peak signal-to-noise ratio (PSNR) by setting a proper Q that serves as a parameter that controls compression (PCC) that can be only integer from 0 to 51 [14].

It is worth stressing that most papers on image lossy compression consider images as noise-free or, at least, pay no attention to possible noise presence in images. Meanwhile, there are numerous reasons why noise can be present in real-life images [6, 15, 16]. Visible noise takes place in optical images if they are acquired in bad illumination conditions [15], in medical and radar images [16] as well as in some components of hyperspectral data [6]. Then, lossy compression irrespectively to a used coder might have two specific phenomena [6, 14, 17]. First, for a rather large CR, a noise filtering effect due to lossy compression exists - this effect was discovered in [16, 17]. Second, the optimal operation point (OOP) that is associated with such PCC that a compressed image is extremely close to the corresponding true (noise-free) image according to a considered similarity metric is possible. It has been shown that both effects can be observed for different coders, various noise types, and different metrics [6, 14, 16-18] including visual quality ones [19, 20].

The OOP existence provides favorable pre-conditions for image compression in OOP or its neighborhood [6, 14, 16]. On the one hand, a rather high quality of the compressed image is provided. On the other hand, a quite large CR is attained. Note that OOP existence and Q for it can be predicted [14, 18] under assumption that noise type and characteristics are a priori known or accurately pre-estimated. If OOP is absent for a given noisy image, it is reasonable to compress such an image with a smaller Q (and, respectively, CR) with introducing less distortions into the image information content [14]. We would like to stress here that, for additive white Gaussian noise (AWGN) considered here for grayscale images, the BPG coder produces better rate-distortion characteristics than other modern coders [21]. This is one more reason for considering the BPG coder.

We have already mentioned that for setting Q that corresponds to OOP one has to know or accurately pre-estimate noise type and characteristics (then, one can use available formulas for setting Q_{OOP} and predicting OOP existence [14, 18]). However, it might be possible that noise characteristics are unknown in advance or it is difficult to estimate them accurately (for example, this happens for highly textural images [22, 23] also called complex structure images). Then, some alternative solution for predicting OOP existence and Q_{OOP} in it as well as assessing image complexity is needed. Note that there exist parameters that can be used for assessment of image complexity [24, 25] but they fail if one deals with noisy images.

Thus, the **object of our study** is the process of lossy compression of noisy images by the BPG-based coder. Our **basic idea** is that the OOP might exist and compression parameters in it can be predicted. **The goal** of this paper is twofold: to design a method for OOP prediction in conditions of limited a priori information on AWGN variance and to analyze ways of complexity assessment for noisy images.

Background of noiseless and noisy image lossy compression

The case of AWGN with zero mean and a priori known variance σ^2 is usually considered as the first step in analysis of many image denoising and lossy compression methods [15, 21, 26]. Also, without losing generality, let us consider conventional 8-bit representation of images and pay the main attention to grayscale ones. Then, the input PSNR is expressed as:

$$PSNR_{inp}=10\log_{10}(255^2/\sigma^2). \quad (1)$$

There are two ways to define PSNR for a lossy compressed noisy image $\mathbf{I_c}$:

$$PSNR_{ct}=10\log_{10}(255^2/MSE_{ct}), \quad (2)$$

$$PSNR_{cn}=10\log_{10}(255^2/MSE_{cn}), \quad (3)$$

where MSE_{ct} and MSE_{cn} are mean square errors determined between the compressed $\mathbf{I_c}$ and noise-free (true) image $\mathbf{I_t}$ and noisy image $\mathbf{I_n}$, respectively. Certainly, the image $\mathbf{I_t}$ is absent in practice (this problem will be discussed later) but one has it in simulations where noise is artificially added to $\mathbf{I_t}$ with obtaining $\mathbf{I_n}$ which is then lossy compressed with obtaining $\mathbf{I_c}$.

If an image is noise-free and it is compressed, one has PSNR that behaves in traditional way, i.e. decreases if PCC (Q in the considered case) increases (see the dependencies in Fig. 1, a for four test images presented in Fig. 2). Note that, in the most important practical interval of Q from 10 to 40, the dependencies are almost linear and "go almost jointly" where PSNR is slightly larger for the simplest structure image Frisco. Fig. 1, b shows the dependencies of $10\log_{10}(CR)$ on Q (logarithmic scale is applied because of two reasons; first, CR (estimated as the ratio of original image size to compressed image size) varies in very wide limits; the second reason will be understood later). As expected, the dependencies are monotonically increasing where the largest CR is for any PCC produced for the simplest structure image Frisco. Also note that, for Q=50, CR exceeds 100 ($1\log_{10}(CR)>2$). Meanwhile, for Q<10, one deals for near-lossless compression.

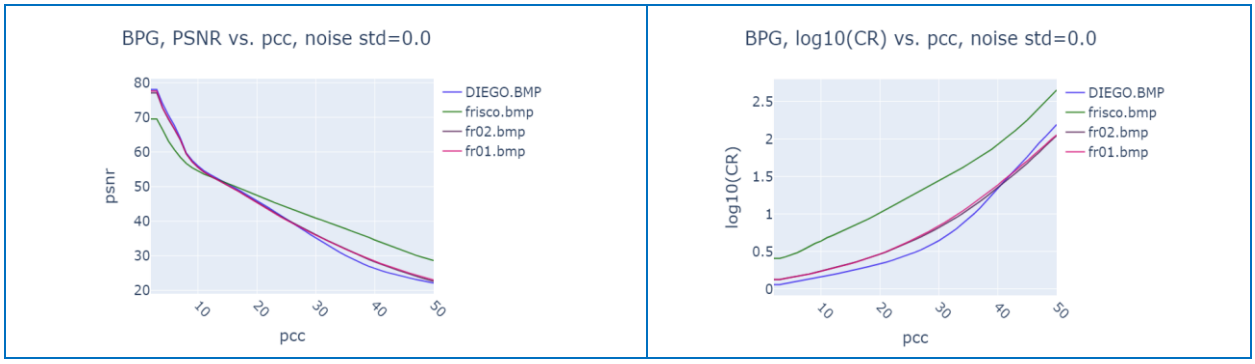

a b

Fig. 1. Dependencies of PSNR calculated between the original noise-free image and its compressed version (a) and dependencies $1\log_{10}(CR)$ on Q (b) for four test grayscale images having different complexity that can be characterized, e.g., by entropy E (smaller entropy corresponds to simpler structure, E=5.82 for the image Frisco and E>7 for three other test images)

a b c d

Fig. 2. Used test images Frisco (a), Fr01 (b), Fr02 (c), and Diego (d)

It is also worth analyzing the dependencies $d(1\log_{10}(CR))/dQ$. They are presented in Fig. 3. Although it seems from visual analysis that the dependencies $1\log_{10}(CR)$ are very smooth (see Fig. 1, b), this is not so and fluctuations are observed. For all four curves and all Q, $d(1\log_{10}(CR))/dQ$ does not exceed 0.1. The derivative $d(1\log_{10}(CR))/dQ$ is the largest for the test image Frisco for Q < 30, but for Q > 30 the derivative $d(1\log(CR))/dQ$ starts to be the largest for the most complex structure image Diego. Thus, having these initial data for analysis, one can expect that behavior and parameters of the curves $d(1\log_{10}(CR))/dQ$ can characterize image complexity (recall that, for lossless compression, CR also depends on entropy characterizing image complexity).

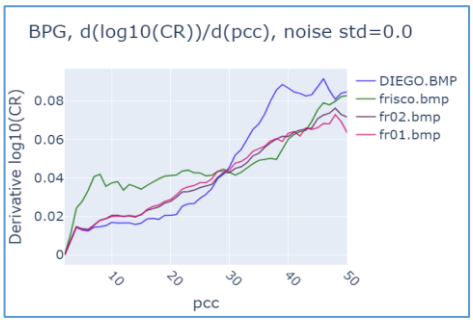

Fig. 3. Dependencies $d(1og_{10}(CR))/dQ$ for noise-free test images

Analysis of the results for noisy test images

Consider now the dependencies for noisy images. Let us start from $\sigma^2 = 25$, i.e. intensity of the noise that can be hardly seen in noisy images. In this case, OOP is obviously observed for the test image Frisco for Q = 30 (Fig. 4, a). Moreover, local maxima take place for the test images Fr01 and Fr02 for the same Q. Only for the test image Diego the dependence is monotonically decreasing and, thus, to avoid undesired distortions of image content, it is reasonable to compress this image using $Q \approx 27$.

Interesting conclusions can be drawn from analysis of dependencies in Fig. 4, b.

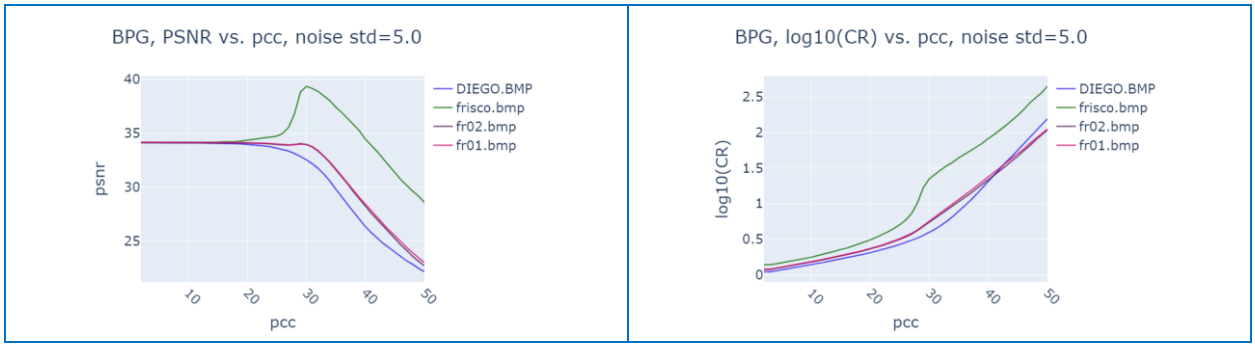

a b

Fig. 4. Dependencies of $PSNR_{ct}$ calculated between the noise-free and compressed noisy images (a) and dependencies $1og_{10}(CR)$ on Q (b) for four test grayscale images having different complexity, $\sigma^2=25$

First, considerably smaller CRs are observed for near-lossless compression ($Q < 10$) of noisy images compared to noise-free ones (compare data in Fig. 4, b and 1, b). This is due to the influence of the noise that is compressed "badly". Second, CR values for large PCC (Q) are almost the same for compressed noisy and noise-free images. This can be explained as follows. For large Q the noise is anyway removed and CR is mainly determined by the image content (complexity). Third, behavior of the curves $1og_{10}(CR)$ on Q for the test image Frisco considerably differs for $Q \approx 30$, i.e. in OOP neighborhood (compare green curves in Fig. 1, b and 4, b). There is a specific inflection area that appears itself in the derivative dependence in Fig. 5 where the derivative maximum exceeds 0.1 and is observed for Q=28. We associate this effect with the fact that the lossy compression starts to suppress noise effectively for Q slightly smaller than Q_{OOP} and this results in fast increasing of CR if Q increases. The results for more intensive noise ($\sigma^2=49$) are presented in Fig. 6. As seen, OOP is observed not only for the simplest structure image Frisco but for the test images Fr01 and Fr02 as well (Fig. 6, a). However, the OOP positions have moved to larger Q ($Q_{OOP} \approx 32$). This not surprising since earlier results [14] have already shown that:

$$Q_{OOP} \approx 14.9 + 10\log_{10}(\sigma^2). \quad (4)$$

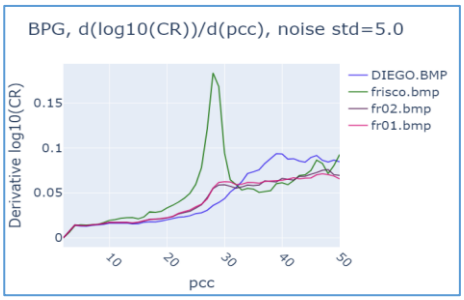

Fig. 5. Dependencies $d(1og_{10}(CR))/dQ$ for noisy test images, $\sigma^2=25$

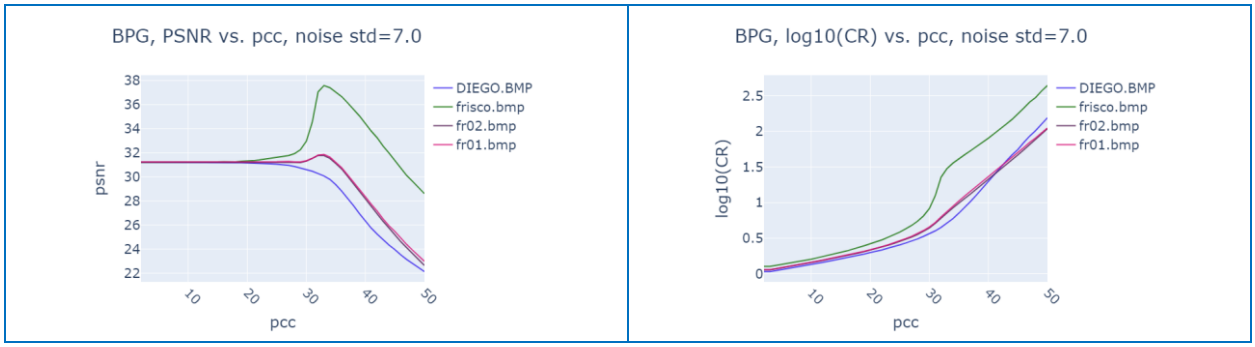

a b

Fig. 6. Dependencies of $PSNR_{ct}$ calculated between the noise-free and compressed noisy images (a) and dependences $1og_{10}(CR)$ on Q (b) for four test grayscale images having different complexity, $\sigma^2=49$

This means that Q_{OOP} for OOP if it exists can be easily determined in advance if σ^2 is a priori known or accurately pre-estimated in advance. However, if one uses inaccurate estimate of σ^2 instead of its true value in (4), Q_{OOP} can be estimated wrongly (with a significant error). The consequences of wrong estimation of Q_{OOP} can be predicted from analysis the dependencies in Fig. 4, a and 6, a. Shifting of Q with respect to the true Q_{OOP} might lead to considerably worse quality of compressed images.

Analysis of the dependencies in Fig. 6, b shows that inflection area exists for the image Frisco and, probably, inflection areas also exist for the test images Fr01 and Fr02. The derivative curves presented in Fig. 7 confirm this. Note that maxima of $d(1og_{10}(CR))/dQ$ for σ^2=49 (Fig.7) have shifted to larger values compared to the case of σ^2=25 and they are observed for $Q_{max} \approx Q_{OOP}$-1.

Consider now the case of σ^2=100. The obtained results are presented in Fig. 8 and 9.

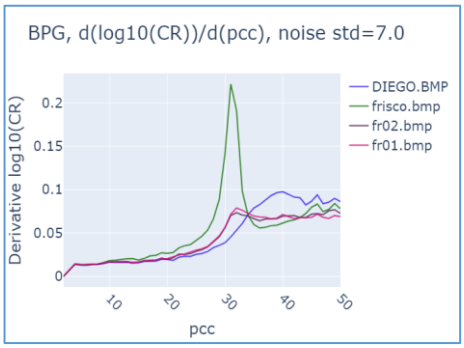

Fig. 7. Dependencies $d(1og_{10}(CR))/dQ$ for noisy test images, σ^2=49

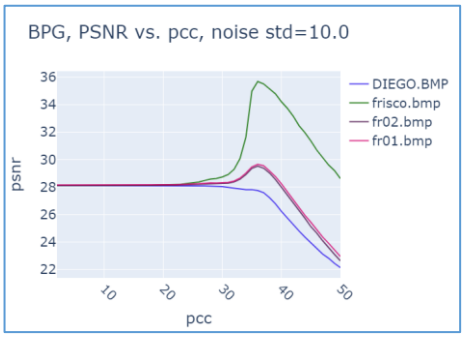

a

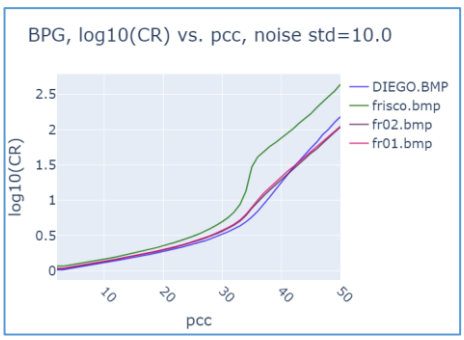

b

Fig. 8. Dependencies of $PSNR_{ct}$ calculated between the noise-free and compressed noisy images (a) and dependencies $1og_{10}(CR)$ on Q (b) for four test grayscale images having different complexity, σ^2=100

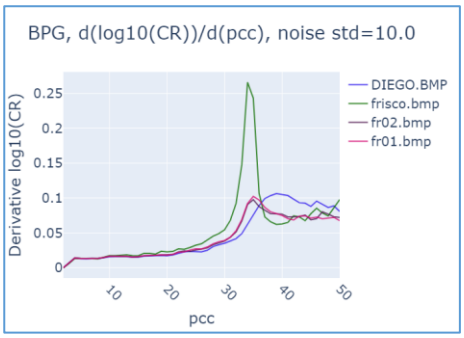

Fig. 9. Dependencies $d(1og_{10}(CR))/dQ$ for noisy test images, σ^2=100

An obvious OOP is observed for the test image Frisco. The OOPs for the test images Fr01 and Fr02 are "less obvious". In all cases, OOPs take place for Q_{OOP}=36 (Fig. 8, a). Inflection points are seen in Fig. 8, b. One maximum exceeding 0.25 and three maxima about 0.1 are observed in Fig. 9.

Finally, the dependencies obtained for σ^2=196 are given in Fig. 10 and 11.

In opposite to previous cases, OOPs are formally observed for all four test images although the OOP for the test image Diego is not obvious (Fig. 10, a). Q_{OOP} has shifted to 39. Inflection points (Fig. 10, b) associated with maxima of $d(1og_{10}(CR))/dQ$ (Fig. 11) are observed as well where Q for inflection points is approximately equal to Q_{OOP}-1.

Let us present the compression results. Fig. 12 shows the noisy Frisco image (Fig. 12, a, AWGN variance is equal to 100, noise is well visible in homogeneous image regions) and three compressed images.

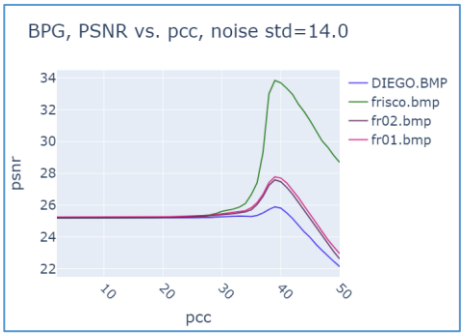

a

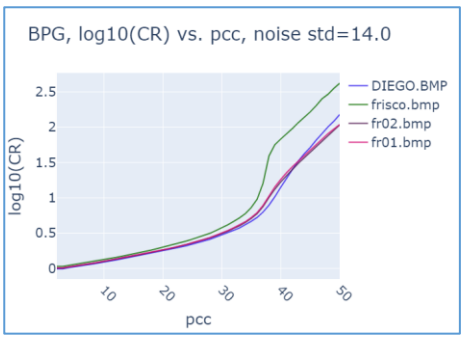

b

Fig. 10. Dependencies of $PSNR_{ct}$ calculated between the noise-free and compressed noisy images (a) and dependencies $1og_{10}(CR)$ on Q (b) for four test grayscale images having different complexity, σ^2=196

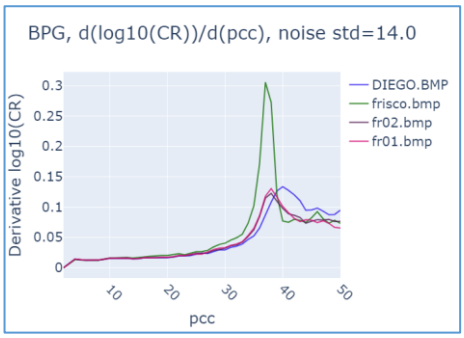

Fig. 11. Dependencies $d(1og_{10}(CR))/dQ$ for noisy test images, $\sigma^2=196$

Fig. 12, b presents the image compressed with $Q_{OOP}=35$ for which CR=29,7, $PSNR_{ct}=35,7$ dB, i.e. CR is quite large and $PSNR_{ct}$ is rather high. Fig. 12, c and 12, d present images compressed with $Q=Q_{OOP}-5=30$ and $Q=Q_{OOP}+5=40$, respectively. In the former case, CR≈5, $PSNR_{ct}=28,7$ dB, i.e. CR and $PSNR_{ct}$ are both worse than for OOP and residual noise is quite intensive. In the latter case (Fig. 12,d), CR (≈78) is larger than in OOP but $PSNR_{ct}$ (≈34.1 dB) is worse, oversmoothing is observed. This example shows advantages of image compression in OOP.

Let us now summarize the obtained results. First, OOP is more probable for simpler structure images and higher intensity noise. If noise intensity increases, Q_{OOP} shifts towards larger values and it can be determined using expression (4) if AWGN variance is a priori known or accurately pre-estimated. Second, if AWGN variance cannot be accurately pre-estimated (this might happen for highly textural images, see below), it is possible to analyze the dependence $d(1og_{10}(CR))/dQ$ with searching for its global maxima and its position. The maximum position is usually connected with OOP as $Q_{max}\approx Q_{OOP}-1$ and, then, Q_{OOP} can be determined as $Q_{max}+1$. Third, if an image has high complexity (and then, OOP is absent or not obvious for any noise intensity), the CR provided for Q=48 is less than 200. This shows that CR(Q=48) is able to characterize image complexity. Fourth, if OOP is obvious in dependencies $PSNR_{ct}$ on Q (that we cannot obtain in practice since $\mathbf{I}_t$ is not available), maximal $d(1og_{10}(CR))/dQ$ exceeds 0.12.

It is also worth taking into account some practical aspects. AWGN is practically invisible in images if σ^2 is smaller than 25 ($Q_{OOP}<29$ if OOP formally exists). Then, there is no reason to look for OOP and it is expedient to set Q=27 or 28 to provide invisibility of distortions. Besides, it is very rare case to have $\sigma^2>200$ and, thus, $Q_{OOP}>39$.

Thus, to minimize time and computational expenses for searching possible OOP, the following procedure can be proposed. Step 1: compress the image with Q=48 and calculate CR. If CR<200, the image is of high complexity and it is not worth searching for OOP for this image. Compress this image using Q=28 as the final step. If CR(Q=48)>200, the following should be done. Compress the considered image using Q from 27 to 40 and calculate $1og_{10}(CR)$ for each Q. Then, obtain $d(1og_{10}(CR))/dQ$ for Q from 28 to 40.

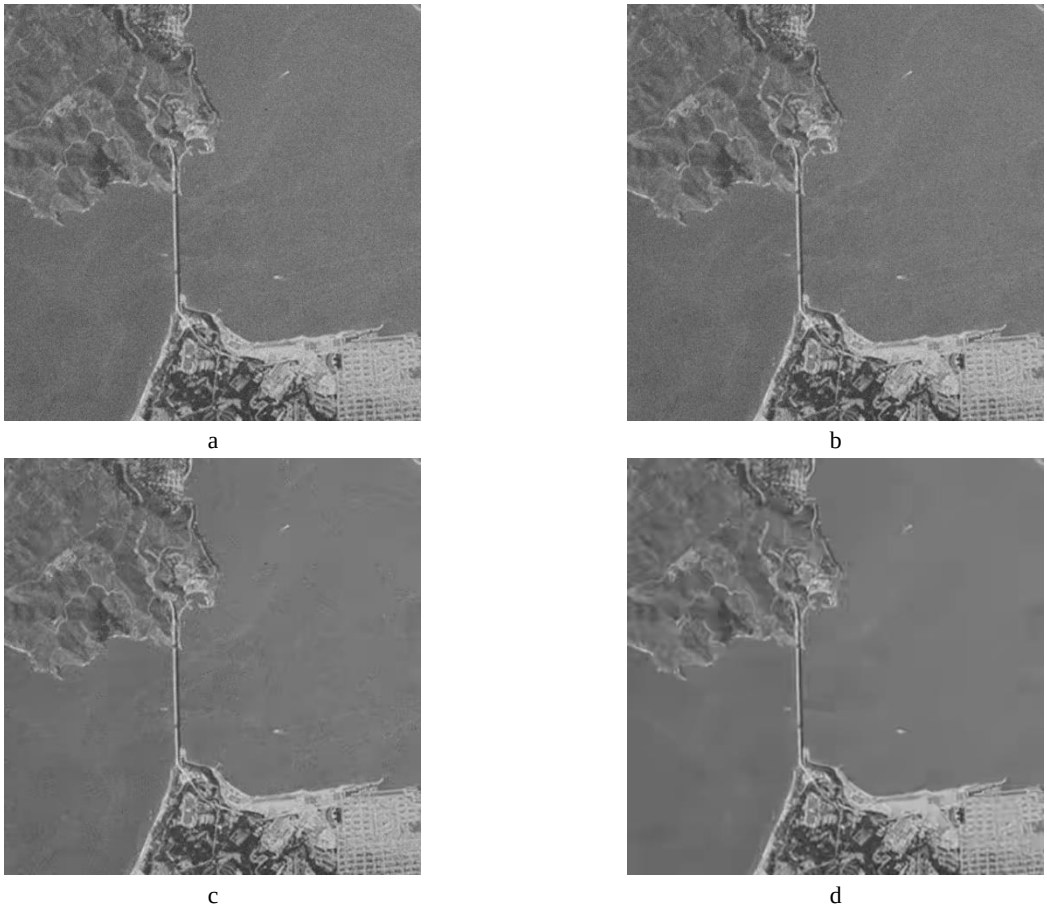

a b c d

Fig. 12. Noisy image Frisco (a) and its compressed versions for $Q=Q_{OOP}=35$ (b), $Q=Q_{OOP}-5=30$ (c) and $Q=Q_{OOP}+5=40$ (d)

If all $d(1og_{10}(CR(Q)))/dQ<0.1$ (as for the plots in Fig. 3), the image is, probably, noise-free and it is worth compressing it using Q=28 to provide invisibility of distortions.

If $d(1og_{10}(CR(Q)))/dQ>0.1+0.003(Q-28)$ for Q from 28 to 40 (the term 0.003(Q-28) is used to take into account the trend of non-informative maximum increasing if Q increases), then find Q_{max} in these limits, and set $Q=Q_{max}+1$ for final compression.

It might seem that such a procedure might take a long time. However, BPG-based compression is quite fast and decompression is not needed.

Besides, there are many cases when only comparison of CR(Q=48) to 200 is needed and then Q for final compression is set equal to 28.

At the moment, we have verified the procedure only for AWGN (several other test images have been analyzed and the obtained results were similar to those presented above). To our opinion, in the future, it is necessary to study the cases of signal-dependent and spatially correlated noise.

Conclusions

In this paper, we have considered behavior of the dependence of CR on Q for the BPG encoder for grayscale images that can be either noise-free or contaminated by AWGN.

It is shown that, although CR(Q) are monotonously increasing dependencies, their analysis allows extracting important information on images and noise.

First, CR for Q approaching 50 allow finding complex structure image for which it is not worth trying to find OOP and compress images in OOP. Second, analysis in the limits from Q=28 to 40 allows getting information on OOP existence and Q_{OOP}. If OOP exists, then it is reasonable to use Q_{OOP} for image compression.

The studies have been carried out for AWGN. More complex noise models are worth studying.

REFERENCES

1. Joshi, N, Baumann, M, Ehammer, A, Fensholt, R, Grogan, K, Hostert, P, Jepsen, M, Kuemmerle, T, Meyfroidt, P, Mitchard, E. and Waske, B. (2016), "A Review of the Application of Optical and Radar Remote Sensing Data Fusion to Land Use Mapping and Monitoring", *Remote Sensing*, vol. 8(1), article number 70, doi: https://doi.org/10.3390/rs8010070
2. Suetens, P. (2017), *Fundamentals of medical imaging*, Third edition, Cambridge University Press, Cambridge, 257 p., available at: https://www.amazon.com/Fundamentals-Medical-Imaging-Paul-Suetens/dp/1107159784
3. Bataeva, E. and Chumakova-Sierova, A. (2022), "Values in Visual Practices of Instagram Network Users", in Integrated Computer Technologies in Mechanical Engineering, Nechyporuk, M., Pavlikov, V., Kritskiy, D. Eds., *Lecture Notes in Networks and Systems*; Springer International Publishing, Cham, vol. 367, number 273869, pp. 992–1002, available at: https://link.springer.com/chapter/10.1007/978-3-030-94259-5_76
4. Stankevich, S.A. and Gerda, M.I. (2020), "Small-size target's automatic detection in multispectral image using equivalence principle", *Cent. Eur. Res. J.*, vol. 6(1), pp. 1–9, available at: https://ceres-journal.eu/download.php?file=2020_01_01.pdf
5. Radosavljević, M., Brkljač, B,. Lugonja, P., Crnojević, V., Trpovski, Ž., Xiong, Z. and Vukobratović, D. (2020), "Lossy Compression of Multispectral Satellite Images with Application to Crop Thematic Mapping: A HEVC Comparative Study", *Remote Sensing*, vol. 12, 1590, doi: https://doi.org/10.3390/rs12101590
6. Zemliachenko, A., Kozhemiakin, R., Uss, M., Abramov, S., Ponomarenko, N., Lukin, V., Vozel, B. and Chehdi, K. (2014), "Lossy compression of hyperspectral images based on noise parameters estimation and variance stabilizing transform", *Journal of Applied Remote Sensing*, vol. 8(1), 25, doi: https://doi.org/10.1117/1.JRS.8.083571
7. Blanes, I., Magli, E. and Serra-Sagrista, J. (2014), "A Tutorial on Image Compression for Optical Space Imaging Systems", *IEEE Geosci. Remote Sens. Mag*., vol. 2, pp. 8–26, doi: 10.1109/MGRS.2014.2352465
8. Hussain, J.A., Al-Fayadh, A. and Radi, N. (2018), "Image compression techniques: A survey in lossless and lossy algorithms", Neurocomputing, vol. 300, pp. 44-69, doi: https://doi.org/10.1016/j.neucom.2018.02.094
9. Bondžulić, B., Stojanović ,N., Petrović, V., Pavlović, B. and Miličević, Z. (2021), "Efficient Prediction of the First Just Noticeable Difference Point for JPEG Compressed Images", *Acta Polytechnica Hungarica*, vol. 18(8), pp. 201–220, doi: https://doi.org/10.12700/APH.18.8.2021.8.11
10. Blau, Y. and Michaeli, T. (2019), "Rethinking lossy compression: The rate-distortion-perception tradeoff", *International Conference on Machine Learning*, PMLR, pp. 675–865, available at: http://proceedings.mlr.press/v97/blau19a.html
11. Bellard, F. (2018), *BPG image format*, available at: http://bellard.org/bpg/
12. Yee, D., Soltaninejad, S., Hazarika, D., Mbuyi, G., Barnwal, R. and Basu, A. (2017), "Medical image compression based on region of interest using better portable graphics (BPG)", *IEEE International Conference on Systems, Man, and Cybernetics* (SMC), pp. 216–221, doi: https://doi.org/10.1109/SMC.2017.8122605
13. Li, F. and Lukin, V. (2023), "Providing a Desired Compression Ratio for Better Portable Graphics Encoder of Color Images", *Design and Analysis, Digitalization and Management Innovation*, Proceedings of DMI 2022, IOS Press, pp. 633–640, doi: https://doi.org/10.3233/FAIA230063
14. Kovalenko, B., Lukin, V., Kryvenko, S., Naumenko, V. and Vozel, B. (2022), "BPG-Based Automatic Lossy Compression of Noisy Images with the Prediction of an Optimal Operation Existence and Its Parameters", *Appl. Sci*., vol. 12, 7555, doi: https://doi.org/10.3390/app12157555
15. Chatterjee, P. and Milanfar, P. (2010), "Is Denoising Dead?", *IEEE Transactions on Image Processing*, vol. 19, no. 4, pp. 895–911, doi: https://doi.org/10.1109/TIP.2009.2037087
16. Al-Chaykh, O.K. and Mersereau, R/M. (1998), "Lossy compression of noisy images", *IEEE Transactions on Image Processing*, vol. 7, is. 12, pp. 1641–1652, doi: https://doi.org/10.1109/83.730376
17. Chang, S., Yu, G. and Vetterli, M. (2000), "Adaptive wavelet thresholding for image denoising and compression", *IEEE Trans. on Image Processing*, vol. 9, is. 9, pp. 1532–1546, doi: https://doi.org/10.1109/83.862633.
18. Kovalenko, B. and Lukin, V. (2023), "BPG-based compression of Poisson noisy images", *Proceedings of DESSERT'2023*, Athens, Greece, 2023, 8 p., doi: https://doi.org/10.1109/DESSERT61349.2023.10416544

19. Wang, Z., Simoncelli, E. P. and Bovik, A. C. (2003), “Multiscale structural similarity for image quality assessment”, *The Thirty-Seventh Asilomar Conference on Signals, Systems & Computers*, vol. 2, pp. 1398–1402, doi: https://doi.org/10.1109/ACSSC.2003.1292216
20. Nafchi, Z. H., Shahkolaei, A., Hedjam, R. and Cheriet, M. (2016), “Mean Deviation Similarity Index: Efficient and Reliable Full-Reference Image Quality Evaluator”, *IEEE Access*, vol. 4, pp. 5579–5590, doi: https://doi.org/10.1109/ACCESS.2016.2604042
21. Kryvenko, S., Lukin, V. and Vozel, B. (2024), “Lossy Compression of Single-channel Noisy Images by Modern Coders”, *Remote Sensing*, vol. 16, doi: https://doi.org/10.3390/rs16122093
22. Abramov, S., Lukin, V., Vozel, B., Chehdi, K. and Astola, J. (2008), “Segmentation-based method for blind evaluation of noise variance in images”, *SPIE Journal on Applied Remote Sensing*, vol. 2, Aug. 2008, 15 p. doi: https://doi.org/10.1117/1.2977788
23. Pyatykh, S., Hesser, J. and Zheng, L. (2013), “Image Noise Level Estimation by Principal Component Analysis”, *IEEE Transactions on Image Processing*, pp. 687–699, doi: https://doi.org/10.1109/TIP.2012.2221728
24. Pavlović, B., Bondžulić, B., Stojanović, N., Petrović, V. and Bujaković D. (2023), “Prediction of the first just noticeable difference point based on simple image features”, *ZINC 2023*, Novi Sad, Serbia, May 29-31, Proc. of papers, pp. 125–130, doi: https://doi.org/10.1109/ZINC58345.2023.10173865
25. Bondžulić, B., Stojanović, N., Lukin, V. and Kryvenko, S. (2024), “JPEG and BPG visually lossless image compression via KonJND-1k database”, *Vojnotehnički glasnik*, Military Technical Courier, vol. 72, no. 3, pp. 1214–1241, 2024, doi: https://doi.org/10.5937/vojtehg72-50300
26. Pogrebnyak, O. and Lukin, V. (2012), “Wiener DCT Based Image Filtering”, *Journal of Electronic Imaging*, no 4, 14 p., doi: https://doi.org/10.1117/1.JEI.21.4.043020

Received (Надійшла) 11.01.2025
Accepted for publication (Прийнята до друку) 09.04.2025

ВІДОМОСТІ ПРО АВТОРІВ/ ABOUT THE AUTHORS

Кривенко Сергій Станіславович – кандидат технічних наук, старший дослідник, докторант кафедри інформаційно-комунікаційних технологій ім. О.О. Зеленського, Національний аерокосмічний університет “ХАІ”, Харків, Україна;
Sergii Kryvenko – Candidate of Technical Sciences, Senior Researcher, Doctoral Student of the Department of Information and Communication Technology, National Aerospace University “KhAI”, Kharkiv, Ukraine;
e-mail: s.kryvenko@khai.edu; ORCID Author ID: https://orcid.org/0000-0001-6027-5442;
Scopus ID: https://www.scopus.com/authid/detail.uri?authorId=59542108400.

Лукін Володимир Васильович – доктор технічних наук, професор, завідувач кафедри інформаційно-комунікаційних технологій ім. О.О. Зеленського, Національний аерокосмічний університет “ХАІ”, Харків, Україна;
Vladimir Lukin – Doctor of Technical Sciences, Professor, Head of the Department of Information and Communication Technology, National Aerospace University “KhAI”, Kharkiv, Ukraine;
e-mail: v.lukin@khai.edu; ORCID Author ID: https://orcid.org/0000-0002-1443-9685;
Scopus ID: https://www.scopus.com/authid/detail.uri?authorId=58857147400.

Бонджуліч Бобан – доктор філософії, доцент, доцент кафедри телекомунікацій та інформатики, Військова Академія, Університет оборони в Белграді, Белград, Сербія;
Boban Bondžulić – PhD, Associate Professor of Department of Telecommunications and Informatics, Military Academy, University of Defence in Belgrade, Belgrade Serbia;
e-mail: bondzulici@yahoo.com; ORCID Author ID: https://orcid.org/0000-0002-8850-9842;
Scopus ID: https://www.scopus.com/authid/detail.uri?authorId=25654605500.

Стояновіч Ненад – аспірант, асистент кафедри телекомунікацій та інформатики, Військова Академія, Університет оборони в Белграді, Белград, Сербія;
Nenad Stojanović – PhD Student, Teaching Assistant of Department of Telecommunications and Informatics, Military Academy, University of Defence in Belgrade, Belgrade Serbia;
e-mail: nenad.m.stojanovic@vs.rs, ORCID Author ID: https://orcid.org/0000-0001-9328-5348;
Scopus ID: https://www.scopus.com/authid/detail.uri?authorId=57205746547.

Стиснення зображень в градаціях сірого з шумом з аналізом коефіцієнта стиснення

С. С. Кривенко, В. В. Лукін, Б. Бонджуліч, Н. Стояновіч

Анотація. Об’єктом дослідження є процес стиснення зашумлених зображень із втратами за допомогою покращеного портативного графічного кодера (BPG). **Предметом** дослідження є метод адаптивного вибору параметра Q кодера залежно від інтенсивності шуму та складності зображення. **Метою** дослідження є розгляд основних характеристик стиснення із втратами зображень дистанційного зондування, спотворених адитивним білим гаусовим шумом, з наданням рекомендацій щодо бажаного налаштування Q. **Використані методи**: чисельне моделювання, перевірка на тестових зображеннях. **Отримані результати**: 1) залежності ступеня стиснення від Q є монотонно зростаючими функціями; 2) їх характеристики сильно залежать від інтенсивності шуму та складності зображення; 3) залежності логарифма CR від Q містять інформацію про можливе існування та положення оптимальної робочої точки для стиснутих зашумлених зображень; 4) коефіцієнти стиснення для великих Q містять інформацію про складність зображення з низькою чутливістю до наявності та інтенсивності шуму; 5) можна отримати корисну інформацію із залежностей ступеня стиснення від Q. **Висновки**: результати цього дослідження дозволяють: 1) оцінити складність зображення; 2) адаптація Q до інтенсивності шуму та складності зображення.

Ключові слова: стиснення з втратами; краща портативна графіка; інтенсивність шуму; складність зображення.